SME Annual Meeting
Feb. 23 - 26, 2014, Salt Lake City, UT

Preprint 14-004

USING NODE ANALYSIS MODELING TECHNIQUES TO PREDICT CAB FILTRATION SYSTEM PERFORMANCE

J. A. Organiscak, NIOSH, Pittsburgh, PA
A. B. Cecala, NIOSH, Pittsburgh, PA
J. D. Noll, NIOSH, Pittsburgh, PA

ABSTRACT

Enclosed cab filtration systems are typically used on mobile mining equipment to reduce miners' exposure to airborne dusts and diesel particulates generated during mining operations. Various filter configurations can be used within the heating, ventilation, and air conditioning (HVAC) systems of cabs to remove the airborne contaminants. The air cleaning performance of cab filtration systems is highly dependent on the efficiency of the air filters, the number of filters used, and their placement within the HVAC system. This paper shows how to mathematically model cab filtration systems and illustrates a methodology for developing other cab filtration system design models. Node diagrams of several filtration system circuits are illustrated with their mathematical models at steady state airflow and concentration conditions. Laboratory and field data are presented to demonstrate the validity and utility of modeling enclosed cab air cleaning performance. The paper concludes that incorporating multiple filters throughout the HVAC system improves the air cleaning performance and robustness of the cab filtration system design.

INTRODUCTION

Enclosed cabs are an engineering control that can provide a safe, comfortable, and healthy worker environment for equipment operators. Most modern day enclosed cabs have heating, ventilation, and air conditioning (HVAC) systems for maintaining a comfortable temperature and a breathable quantity of air for their occupants. Various levels of filtration can be incorporated into the HVAC system to improve the ventilation quality of the air inside the cab by removing airborne pollutants such as dusts and diesel particulates. Previous enclosed cab dust filtration system field studies were conducted by the National Institute for Occupational Safety and Health (NIOSH) at mining operations, and these studies showed that the respirable dust reduction or protection factors (outside/inside concentrations) ranged from 3 to 89 (Organiscak et al. 2004; Chekan and Colinet 2003; Cecala et al. 2004; Cecala et al. 2005; Cecala et al. 2012-A). The two key components attributed to the more effective cab dust control results were an efficient filtration system and an effectively sealed cab (good cab integrity) for achieving positive interior pressurization (Cecala et al., 2013).

Previous laboratory experiments were conducted to methodically study the key design factors of effective cab filtration systems. These laboratory experiments examined the effects of intake filter efficiency, intake filter loading, intake air leakage around the filter, recirculation filter use, and wind on cab filtration system performance (Organiscak and Cecala 2008-A; Organiscak and Cecala 2008-B). The experimental cab test results showed that intake filter efficiency and recirculation filter use were the two most important influential factors on cab filtration system penetration performance. The addition of a recirculation filter to the cab's filtration system significantly reduced its particulate penetration by an order of magnitude and reduced the time to reach its lowest stable concentration after the entrance door was closed by approximately 60%. Finally, a mathematical model was developed that describes cab particulate penetration in terms of intake filter efficiency, intake air quantity, intake air leakage, recirculation filter efficiency, recirculation filter quantity, and wind penetration (Organiscak and Cecala 2008-B).

The enclosed cab filtration systems previously studied by NIOSH on mine vehicles during field evaluations filtered both the HVAC intake and recirculation airflows. Several of these cab filtration system systems also incorporated a third final filter downstream of the intake and recirculation filters (Chekan and Colinet 2003; Cecala et al. 2004; Cecala et al. 2012-A). The most recent field study of two underground limestone mine vehicle cabs (face drill and roof bolter) that used a three-filter HVAC system design (intake, recirculation, and final filters) provided protection factors greater than 1,000 on submicron particles (0.3 to 1.0 µm), measured with particle counters after steady state interior cab concentration was reached (Cecala et al. 2012-A). These high cab protection factors were regularly attained over an extensive range of intake and recirculation airflows measured during a seven-month field study. Since the mathematical model previously formulated from the laboratory study for a two-filter system (intake and recirculation filter) cannot be applied in its current form to examine the performance range of this three-filter system design (intake, recirculation, and final filter), a new three-filter cab filtration model was devised. The objective of this paper is to illustrate a methodology to formulate cab filtration system models and verify their utility in designing and predicting cab performance from field and laboratory data.

MODELING METHODOLOGY

The two-filter cab filtration model previously developed was a time-related mass balance (differential equation) inside a control volume (cab) that was converged to a steady state solution as time approached infinity (Organiscak and Cecala 2008-B). The methodology that was used and illustrated in formulating a three-filter model is a mass balance of contaminants in a cab filtration circuit at steady state conditions. Steady state conditions are the lowest contaminant concentrations achievable inside the cab at constant outside contaminant concentrations and filtration system airflow quantities. This simplifies the model development to drawing out a node diagram of airflow circuit for the filtration system, devising the mass flow equation into and out of the node inside the cab, and algebraically solving the mass flow equation for the ratio of the outside concentration entering and leaving the cab filtration system.

Mathematical Formulation of Cab Filtration Systems

Figure 1 illustrates the node diagram of the three-filter system used and studied on vehicle cabs in an underground limestone mine (Cecala et al. 2012-A). As shown, in this particular filtration system the final filter is downstream of the intake and recirculation filters. Outside contaminants enter into the filtration system circuit through the intake filter, leakage around the intake filter, and direct penetration into the cab enclosure openings when wind velocity pressure exceeds cab pressure. Some of the filtered interior cab air is pushed outside by the intake airflow and any outside wind penetration, while the remaining portion of the cabin air is recirculated through the recirculation and final filters. The filtration system model is formulated as an equality of the incoming contamination mass to the exiting contamination mass at the interior cab node as defined in equation 1:

$$Mass_{in} = Mass_{out} \quad (1)$$

Additional contaminants can be brought into the cab enclosure on worker clothing and boots and later generated inside the cab interior

through worker activities; however, development of this model primarily focuses on outside airborne contaminants that penetrate the cab filtration system, excluding worker-generated sources.

The incoming mass is what penetrates the cab filtration system and the outgoing mass is what leaves the cab interior and is recirculated through the filtration system as shown in equation 2:

$$\left[CQ_i(1-\eta_I)+CQ_L+xQ_R(1-\eta_R)\right](1-\eta_F)+CQ_W = x(Q_I+Q_W)+xQ_R \quad (2)$$

where:

C = outside contaminant concentration penetrating the filtration system,
x = inside cab contaminant concentration (interior cab node),
η = filter reduction efficiency, fractional,
1-*η* = filter penetration, fractional,
Q = airflow quantity,
l = intake air leakage, fractional,

with filter efficiency and air quantity subscripts:

i - filtered intake air,
F - final
I - intake,
L - leakage,
R - recirculation,
W - wind

Since $Q_I = Q_L + Q_i$ and $Q_L = Q_I\, l$, the substitutions of $Q_i = Q_I(1-l)$ and $Q_L = Q_I\, l$ are made into equation 2:

$$\left[CQ_I(1-l)(1-\eta_I)+CQ_I\, l+xQ_R(1-\eta_R)\right](1-\eta_F)+CQ_W = x(Q_I+Q_W)+xQ_R \quad (3)$$

The terms within the brackets are multiplied and simplified:

$$\left[CQ_I\,(1-\eta_I+l\eta_I)+xQ_R-xQ_R\eta_R\right](1-\eta_F)+CQ_W = x(Q_I+Q_W)+xQ_R \quad (4)$$

The bracketed intake and recirculation terms are multiplied by the final filter penetration term:

$$\left[CQ_I\,(1-\eta_I+l\eta_I)(1-\eta_F)\right]+xQ_R-xQ_R\eta_F-xQ_R\eta_R+xQ_R\eta_R\eta_F+CQ_W = x(Q_I+Q_W)+xQ_R \quad (5)$$

The outside and inside concentration terms are rearranged to opposing sides of the equation:

$$CQ_I(1-\eta_I+l\eta_I)(1-\eta_F)+CQ_W = x(Q_I+Q_W)+xQ_R\eta_F+xQ_R\eta_R-xQ_R\eta_R\eta_F \quad (6)$$

which simplified and rearranged results in:

$$C\left[Q_I(1-\eta_I+l\eta_I)(1-\eta_F)+Q_W\right] = x\left[Q_I+Q_R(\eta_R+\eta_F-\eta_R\eta_F)+Q_W\right] \quad (7)$$

Next, we solve for protection factor (PF) ratio or penetration (Pen = 1/PF). The equation below was solved for protection factor and can easily be inverted to determine penetration:

$$PF = \frac{C}{x} = \frac{Q_I+Q_R(\eta_R+\eta_F-\eta_R\eta_F)+Q_W}{Q_I(1-\eta_I+l\eta_I)(1-\eta_F)+Q_W} = \frac{1}{Pen},$$

for the three-filter model (8)

This equation can be reduced to a two-filter model (intake and recirculation filter only) as shown in Figure 2 by substituting zero for the final filter efficiency. The equation can also be reduced to a single-intake filter model as shown in Figure 3 by substituting zeroes for the final and recirculation filters. These reduced models are shown below. The wind penetration quantity into the cab is zero ($Q_W = 0$) for all these models when the interior cab pressure is greater than the exterior wind velocity pressure.

$$PF = \frac{C}{x} = \frac{Q_I+Q_R\eta_R+Q_W}{Q_I(1-\eta_I+l\eta_I)+Q_W} = \frac{1}{Pen},$$

for the two-filter model without final filter (9)

$$PF = \frac{C}{x} = \frac{Q_I+Q_W}{Q_I(1-\eta_I+l\eta_I)+Q_W} = \frac{1}{Pen},$$

for the single-intake filter model (10)

Note: In the previously formulated two-filter model (intake and recirculation filter), the wind penetration airflow (Q_W) was only accounted for as incoming mass concentration (*C*) into the cab (Organiscak and Cecala 2008-B). As an oversight in its development, the outgoing mass concentration (*x*) from wind penetration (Q_W) was not included in that model and does not appear in both the numerator and denominator of that model. However, when the cab enclosure is adequately pressurized at or greater than the exterior wind velocity pressure, the wind penetration airflow (Q_W) can be considered to be negligible or zero and the models agree. For particular situations like an open door, open window, or poorly sealed cab with no cab pressure, notable quantities of air can penetrate the cab enclosure from the outside and equations 8, 9, and 10 would more accurately represent these types of conditions.

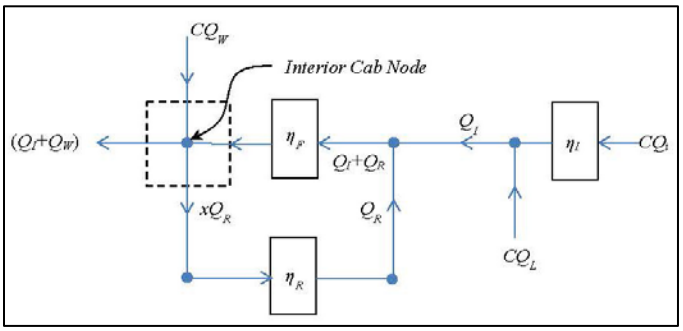

Figure 1. Three-filter cab system with final filter downstream of intake and recirculation filters (*Q*'s denote air quantities, *x*'s & *C*'s denote contaminant concentrations, and *η*'s denote filter efficiencies).

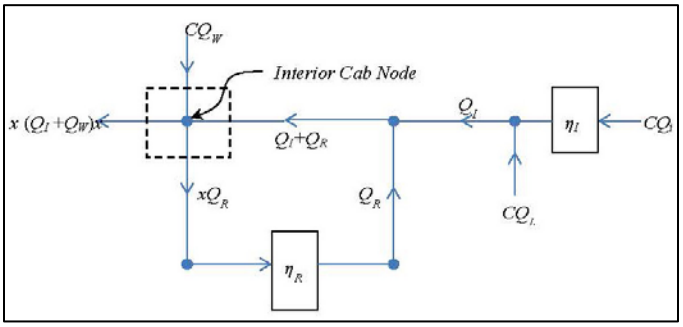

Figure 2. Two-filter cab system with intake and recirculation filters (*Q*'s denote air quantities, *x*'s & *C*'s denote contaminant concentrations, and *η*'s denote filter efficiencies).

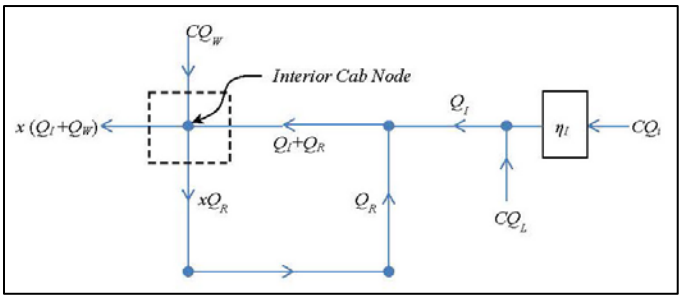

Figure 3. Single-intake filter cab system (*Q*'s denote air quantities, *x*'s & *C*'s denote contaminant concentrations, and *η*'s denote filter efficiencies).

CAB PERFORMANCE MEASUREMENTS

In order to authenticate the cab filtration system models, airflow quantities, filter efficiencies, and cab airborne particulate reductions

must be measured at or near steady state conditions in an unoccupied cab. These types of cab measurements were initially conducted in the laboratory on NIOSH's experimental cab test apparatus for single- and two-filter systems (Organiscak and Cecala 2008-A; Organiscak and Cecala 2008-B). A three-filter cab system design was more recently studied on underground limestone face drill and roof bolter cabs over a seven-month period. Airflow and particle counting measurements were completed between production shifts on the surface (Cecala et al. 2012-A). Since filter efficiencies cannot easily be measured in the field, the known or specified filter efficiencies were used for the mathematical modeling, while the unspecified filters were tested in the lab on NIOSH's experimental cab test apparatus to determine their filter efficiencies.

Particle Counting Measurements

The cabs' protection factors were measured by using two model ARTI/Met One HHPC-6 particle counters (Hach Ultra Analytics, Grants Pass, OR) to simultaneously sample and record the inside and outside cab particle size concentrations for one-minute periods over a 30-minute test (with a recirculation filter) or a 45-minute test (without a recirculation filter), as previously discussed for NIOSH's laboratory cab experiments (Organiscak and Cecala 2008-A; Organiscak and Cecala 2008-B). These instruments count airborne particles within the six-channel size ranges of 0.3-0.5 µm, 0.5-0.7 µm, 0.7-1.0 µm, 1.0-3.0 µm, 3.0-5.0 µm, and > 5.0 µm. The test medium was airborne particles present in the ambient air surrounding the unoccupied stationary cab enclosure with the filtration system operating. The inside and outside cab instruments were alternated for an equal number of test replicates and were expected to average out any instrument sampling biases between the tests. At least four test replicates were conducted during each of the laboratory test conditions but only two test replicates were conducted during the field studies given the time constraints at the mine site. The last 15 minutes of data from each test replicate were used to calculate the average outside and inside cab concentrations during the lowest steady state particle count conditions inside the cab. The protection factors were determined from the cumulative submicron (0.3-1.0 µm) particle concentrations because most of the ambient air particles resided in this size range. A protection factor for each test replicate was determined by dividing the average outside particle concentration by the average inside particle concentration with the replicates averaged for the cab protection factor at the operating test condition. The protection factor represents a reduction ratio of all the exterior and interior particles removed by the cab filtration system.

The submicron particle (0.3-1.0 µm) collection efficiencies of the filters used in the laboratory experiments were also measured with MetOne HHPC-6 particle counters immediately upstream and downstream of the filter on NIOSH's experimental cab test apparatus. Intake filter efficiencies were concurrently measured during each cab test by sampling downstream of the filter with a third MetOne particle counter (Organiscak and Cecala 2008-B). The recirculation filter efficiency was measured separately from the laboratory cab tests by sampling immediately upstream of the filter with an open cab door and iso-kinetically sampling immediately downstream of the filter in the recirculation ductwork with the intake air ducts closed (Organiscak and Cecala 2008-B). The recirculation filter tests were conducted at a comparable airflow quantity to the experimental laboratory tests that were used to quantify cab protection factors. Eight 15-minute test replicates were conducted with two particle counters, rotated between the upstream and downstream sampling locations during each test.

Independent filter tests were also conducted on NIOSH's experimental cab test apparatus with the unrated intake and recirculation filters (pre-filters) used in the field study for the three-filter system. The final filter and one of the intake filters used during the field studies had an American Society of Heating, Refrigerating and Air-Conditioning Engineers (ASHRAE) minimum efficiency reporting value of 16 (MERV 16, efficiency > 95% down to 0.3 µm particle sizes)(ASHRAE, 1999). The MERV 16 final filters and unrated recirculation filters were used in the two cab filtration systems field tested, with one of the cabs using an unrated intake filter and the other cab using a MERV 16 intake filter. A more detailed description of the filters used in the field study can be found in Cecala et al. 2012-A. The unrated recirculation and intake filters (no ASHRAE MERV rating) used upstream of the MERV 16 final filter during the field study were tested in the laboratory for their submicron collection efficiency. Each of these filters was separately tested in a new and used (dust-loaded) condition with MetOne HHPC-6 particle counters on NIOSH's experimental cab test apparatus. Eight 15-minute test replicates were conducted with two particle counters, rotated between the upstream and downstream sampling locations during each test condition at comparable airflows observed in the field. Filter efficiencies were determined for each test condition and averaged for the eight test replicates to estimate the low and high range of filter efficiencies during the long-term field study.

Airflow and Cab Pressure Measurements

Airflow readings were measured for the intake and recirculation circuits of the cab enclosures' filtration system to examine the cab operating effects of different filter combinations. For NIOSH's experimental cab test apparatus, the intake airflow velocity was centerline measured inside the 3-in.-dia. PVC intake pipe with a TSI Model 8346 VelociCALC Hot Wire Anemometer (TSI, Inc., Shoreview, MN). The recirculation airflow was measured with an ALNOR Standard Balometer Capture Hood (TSI, Inc., Alnor Products, Shoreview, MN) placed over the inlet side of the recirculation filter. The experimentally controlled air leakage path bypassing the intake filter was measured with a TSI Model 4040 Thermal Mass Flowmeter (TSI, Inc., Shoreview, MN). During the field study, VELOCICALC hotwire anemometer models 8346 or 9555 (TSI Incorporated, Shoreview, MN) were used to measure the centerline air velocity inside the middle of a 122-cm-long (4-ft-long) section of smooth 10.2-cm-dia. (4-in.-dia.) PVC pipe which was added to the inlet of the intake filtering unit. For the recirculation component, one-minute moving traverse velocity measurements were made with a vane anemometer (Davis Instruments, Vernon Hills, IL) over the recirculation filter inlet area. A more detailed description of these measurements can be found in Organiscak and Cecala 2008-B and Cecala et al. 2012-A.

The cab's inside to outside differential static pressure was also measured in the laboratory and field to ensure that cab pressurization was achieved. Cab pressure measurements were taken with either a 0.0-125 Pa (0.0-0.5 in. water gauge) Magnehelic differential pressure instrument (Dwyer Instruments, Inc., Michigan City, IN) or a DP-CALC Model 5825 Micromanometer (TSI, Incorporated, Shoreview, MN).

CAB FILTRATION SYSTEM PERFORMANCE RESULTS

The laboratory and field cab filtration system protection factor measurements were compared to those modeled from filter efficiencies, airflow quantities, and fractional air leakages measured at various test conditions. During the laboratory experiments, almost all of the model variables were directly measured during the test conditions with the exception of the recirculation filter efficiency which was measured separately from the cab testing. Therefore, the laboratory filtration system protection factor measurements can be directly plotted against the modeled results. During field testing, the three-filter efficiencies changed with filter dust loading as indicated by the reduction in intake and recirculation airflow quantities and the increase in protection factors measured during the study (Cecala et al. 2012-A). Given filter efficiency changes with dust loading, the three-filter cab filtration system was modeled for a lower and upper limit curve at the various recirculation to intake airflow ratios measured in the field with new and used (loaded) filters. The two cabs' protection factor measurements were plotted at the various recirculation-to-intake airflow ratios to verify if the field results were within the models' predicted lower and upper operating ranges.

Laboratory Results

Figure 4 shows an x-y plot of the measured and modeled protection factors for a single-intake filter system (equation 10) and a two-filter system (equation 9), with an intake and recirculation filter. This figure plots the average measured cab protection factors (x-axis) versus the modeled protection factors (y-axis), using the average cab operating variables measured at the different intake and recirculation filter conditions reported from the laboratory experiments (Organiscak and Cecala 2008-A; Organiscak and Cecala 2008-B). As illustrated in this graph, there is good positive correlation (correlation coefficient, r =

0.995 at significance level, $p < 0.02$) between the measured and modeled cab protection factors. A notable difference in protection factors was also observed between the two intake filters tested (filter efficiencies, $\eta_I < 40\%$ and $\eta_I > 99\%$) and when the recirculation filter ($\eta_R = 72\%$ efficiency) was added to the filtration system. Therefore, filter efficiency and the number of filters used in the filtration system had a significant effect on cab protection factor performance and can be reasonably modeled at steady state operating conditions, knowing the filter efficiencies, system airflow quantities, and air leakage bypassing the intake filter.

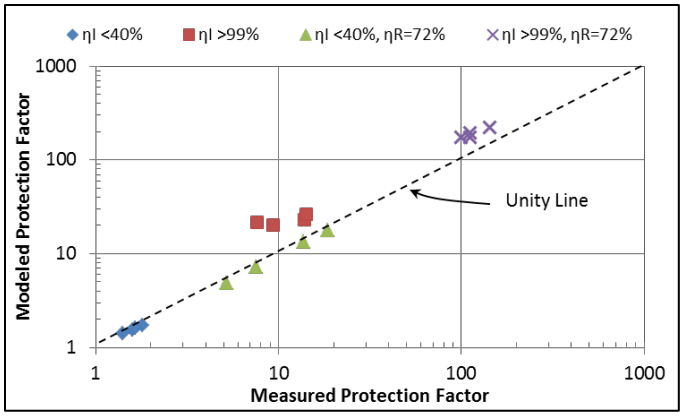

Figure 4. Comparison of laboratory measured cab protection factors to the modeled protection factors.

Field Results

Cab protection factor modeling was conducted using new and used filter efficiencies over the range of recirculation to intake airflow ratios measured during the field studies (Cecala et al. 2012-A). Table 1 shows the laboratory testing conditions for the unrated intake and recirculation filters and their respective submicron (0.3-1.0 µm) collection efficiencies measured for modeling cab protection factor performance thresholds during field testing. The intake filter airflow rate tested was similar to the average airflow rate measured on the face drill in the field (Cecala et al. 2012-A). The recirculation airflow rates tested were similar to the airflow rates measured within the first few shifts with a new filter and within the last few shifts just before the filter was changed (Cecala et al. 2012-A). The particle size collection efficiency characteristics measured for both these unrated intake and recirculation filters used during the field testing are also shown in Figure 5. As can be seen in this illustration, the filter efficiencies notably increased from the new filter condition to the used (loaded) filter condition. The intake filter collection efficiency for submicron particles (0.3-1.0 µm) increased from 23% to 98% for the new and used filter, respectively. The recirculation filter collection efficiency for submicron particles (0.3-1.0 µm) increased from 12% to 76% for the new and used filter, respectively. These filters were used as pre-filters placed upstream of the higher efficiency MERV 16 final filter used in the face drill cab filtration system.

Table 1. Intake and recirculation filter test conditions and collection efficiency results, average [range].

Unrated Filters Tested	Filter Condition (new/used)	Filter Airflow (m^3/hr)	Differential Pressure (Pascals)	Filter Efficiency for 0.3–1.0 µm Particles (fractional)
Intake filter	New	120 [119–121]	62.3	0.228 [0.188–0.262]
Intake filter	Used	119 [118–120]	433	0.984 [0.983–0.984]
Recirculation Filter	New	301 [294–308]	[261–273]	0.119 [0.082–0.142]
Recirculation Filter	Used	81.7 [77.1–86.1]	[336–348]	0.761 [0.751–0.767]

The MERV 16 final filters used on both cab filtration systems and the MERV 16 intake filter used on the pressurizer intake unit of the bolting machine cab were both rated at greater than or equal to 95% collection efficiency on submicron particles (0.3-1.0 µm). For protection factor modeling, these filters will be assumed to be 95% efficient at their new condition and at least 98% efficient in their loaded condition, similar to the loaded intake filter efficiency measured in the laboratory. The only difference between the cab filtration systems tested during field evaluations was that the roof bolter cab had a fan-powered pre-cleaner pressurizer unit with the MERV 16 intake filter compared to an unpowered intake filter unit with the unrated intake filter used on the face drill cab. The final and recirculation filters used on both cabs were the same throughout most of the field testing, having similar intake and recirculation airflow rates during field testing (Cecala et al. 2012-A). After approximately 500 hours of operation, or 2/3s of the bolter testing period, the recirculation filter was removed to examine the operational effectiveness of this two-filter system configuration (MERV 16 intake and final filter) when using the pressurizer intake unit (Cecala et al. 2012-A). Using the two-filter configuration on the bolting machine dramatically increased its filtration system recirculation airflow rate during the latter part of the field tests. The face drill cab testing throughout the field study continued to use the three-filter configuration, because the unpowered intake filter unit only provided negligible intake airflow into the cab with the recirculation filter removed (Cecala et al. 2012-A).

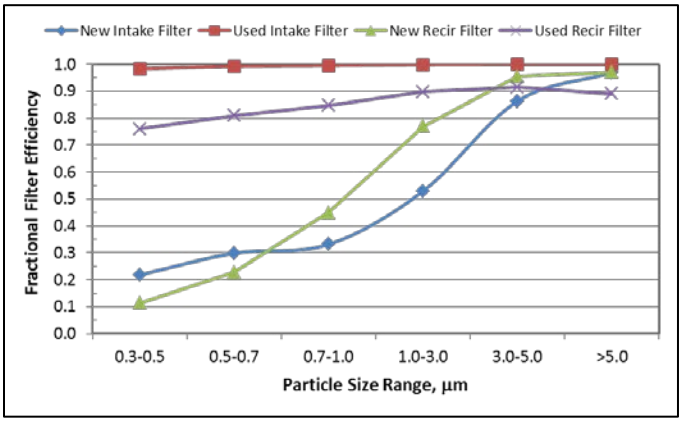

Figure 5. Intake and recirculation pre-filter particle size efficiency measurements.

Figure 6 shows the cab protection factors measured during the field studies as compared to the expected lower (blue solid) and upper (green solid) operating ranges modeled for the cab filtration systems. The three-filter cab modeled (equation 8) used 119 m^3/hr (70 ft^3/min) of intake airflow with recirculation airflows ranging between 42.5 and 680 m^3/hr (25 to 400 ft^3/min), at an assumed 2% (0.02) intake air leak, and with no wind penetration. The assumed 2% (0.02) intake airflow leakage was used for all the field cab modeling because others have considered this figure to be the maximum amount of leakage acceptable for a sufficiently sealed cab filtration system (ASAE 1997). The lower protection factor model curve was determined with the new intake and recirculation fractional filter efficiencies of 0.23 and 0.12, respectively (see Table 1), and a new final filter efficiency of 0.95. The upper protection factor model curve was determined with the used intake and recirculation filter efficiencies of 0.98 and 0.76, respectively (see Table 1), and a used final filter efficiency of 0.98. Figure 6 illustrates that 29 out of 33 field protection factor measurements were found to be within the modeled operating ranges (curves) expected from these cab filtration systems. The cab measured points were spread out between the lower and upper model curves because both the filter efficiencies and airflows were changing due to dust loading over the seven-month sampling period (Cecala et al. 2012-A). The four outlying points can simply be accounted for by slightly increasing or decreasing the model's filter collection efficiencies by 1 to 2% (0.01 to 0.02) or the intake leakage value by 1 to 2% (0.01 to 0.02). It is reasonable to expect that these filter efficiencies and leakage values can vary by this much due to filter product variations, filter airflow efficiency variations, and diverse dust loading conditions experienced between cabs during mining. Operating the roof bolter filtration system without the recirculation filter (open points in figure 6) increased the recirculation to intake airflow ratio while maintaining comparable

protection factors with the three-filter system. This particular two-filter system arrangement performed well because the high efficiency final filter cleans both the filtered intake air and unfiltered recirculation air.

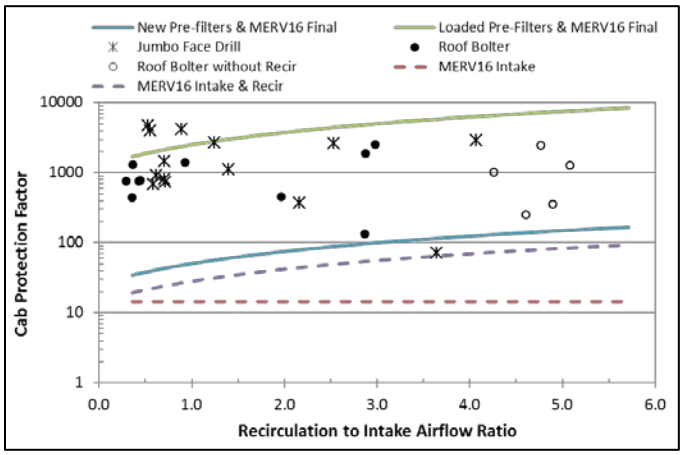

Figure 6. Field-measured protection factors shown with modeled ranges.

Finally, a single- and two-filter system (equations 10 and 9), without a final filter were modeled with their curves also shown in Figure 6. The first curve (red dashed) was modeled using only a new MERV 16 rated (95%) intake filter and the second curve (purple dashed) was modeled using both a new MERV 16 rated (95%) intake and recirculation filter. These models used identical airflow and leakage operating conditions as the three-filter systems modeled with a final filter. The single-intake MERV 16 filter model shows a constant protection factor of 14.5 for the recirculation to intake airflow ratio range modeled. The two-filter system model illustrates a progressively higher cab protection factor with respect to the recirculation to intake airflow ratio as compared to the single-intake filter model. This improvement is a result of the multiplicative filtration of the cab's interior air (Organiscak and Cecala 2008-B). The three-filter system (models and field data) with a MERV 16 final filter was shown to perform better than the single- and two-filter models with MERV 16 filters because the final filter additionally cleans all the air circulated throughout the cab filtration system. Comparing the field data in Figure 6 to the laboratory data in Figure 4 shows that the three-filter system with a final filter can outperform a two-filter system without a final filter.

DISCUSSION

The single-, two-, and three-filter system models described in this paper are only a few of many that can be developed by using the node analysis technique. In particular, air leakage was only introduced and modeled as outside air bypassing the intake filter. Air leakage around other filters in the system can also be quantified by multiplying the filter penetration (1 - η) by the portion of airflow passing through the filter (1 - I), as previously demonstrated for the intake air leakage term in equation 3. Intake air leakage was specifically modeled by the authors because contaminant concentrations are usually the highest outside the cab and their leakage around the intake filter would most likely impact the response of the system models. Also, the largest negative pressure differential in the filtration system with respect to atmospheric pressure is usually at the outside intake filter unit, increasing the likelihood of air leakage through the intake circuit of the system. Other filtration system designs can be conceived and modeled by similarly applying these node analysis techniques demonstrated.

Most of the cab filtration modeling exercises described in previous publications and in this paper assume adequate cab enclosure pressurization with no outside wind intrusion into the cab (Cecala et al. 2013; Cecala et al. 2012-B; Organiscak and Cecala 2009). The quantity of wind infiltration into cab enclosures with very low to no pressure is difficult to directly measure and has been previously estimated by defining the operating conditions with orifice airflow exiting the cab being reversed to orifice airflow into the cab (Heitbrink et al. 2000; Organiscak and Cecala 2008-B). This tends to occur when wind air velocity pressure exceeds cab static pressure. Exterior wind infiltration into an enclosure was previously related to the wind velocity pressure and static cab pressure differential across round orifices in an enclosure facing directly into the wind (Heitbrink et al. 2000). Given that wind airflow intrusion through other cab opening configurations (orifice shapes, orientations, shielded, etc.) can be more difficult to predict, and that numerous gaps or holes in cab enclosures are typically concealed, accurate wind airflow quantities infiltrating most cabs would be nearly impossible to determine at very low to no cab pressures. However, a cab with good enclosure integrity can typically be pressurized above wind velocity pressures to ensure that maximum cab protection factor performance of the filtration system can be achieved. A reasonable operating range of cab enclosure pressures is between 12.5 and 62.3 Pa (0.05 and 0.25 inches wg.), which should withstand wind velocity intrusions of 16.4 and 36.5 km/hr (10.2 and 22.7 miles/hr), respectively (Cecala et al. 2013; Cecala et al. 2012-B).

Figure 7 illustrates the detrimental effects that wind infiltration into the cab can have on protection factors by modeling a range of wind to intake airflow infiltration into the cab enclosure at two particular operating conditions. The cab filtration system modeled was the three-filter system using new and used intake, recirculation, and MERV 16 final filters. Table 1 shows the intake and recirculation filter efficiencies and their airflow conditions modeled, assuming a 2% intake airflow leakage. The new and used MERV 16 final filter efficiencies also used in these models were 0.95 and 0.98, respectively. Minimal cab protection factor changes were projected below one-thousandth (0.001) of the wind to intake airflow ratio infiltrating the cab, while noticeable protection factor decreases were projected above this airflow ratio. Although the cab with higher efficiency filters performed notably better than the cab with lower efficiency filters at minimal wind intrusion, the performance deteriorated more rapidly as wind infiltration increased and became worse than the lower efficiency filter cab when the wind to intake airflow ratio was above 0.03. This noteworthy cab performance change with the higher efficiency filters was a result of the wind infiltration into the cab being filtered at a lower recirculation airflow rate than the cab with the lower efficiency filters. The significant deterioration in cab protection factors illustrated for both cabs above the wind to intake airflow ratios of 0.10 would likely represent a condition where a door or window would be open. These significant deteriorations in cab performance when doors are opened have been observed and measured in previous field studies (Noll et al. 2010, NIOSH 2008).

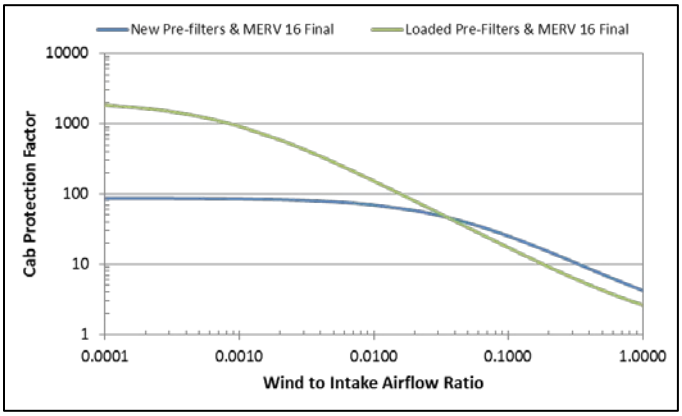

Figure 7. Detrimental wind infiltration effects from very low to no cab enclosure pressurization.

CONCLUSIONS

Node analysis modeling techniques were used to describe the performance of cab filtration systems and were verified by laboratory and field testing of these systems. A node diagram of a three-filter system was illustrated with the formulation of a mathematical model that described the mass concentration balance removed by the cab filtration system and leaving the cab enclosure at steady state conditions. Model variables included filter efficiencies, intake airflow, intake airflow leakage, recirculation airflow, and wind infiltration airflow.

This three-filter model was further reduced to a two-filtration system model by substituting zero for the final filter in the system and a one-cab filtration system by substituting zeros for the final and recirculation filters in the system. The laboratory cab protection factor performance data for a single-filter (intake) and two-filter (intake and recirculation) systems had a good correlation coefficient of 0.995 (significance level < 0.02) with the protection factor performance model of the filter system operating parameters.

For the three-filter model verification of the cab field data collected, new and used intake and recirculation filters had to be laboratory tested to determine their submicron (0.3-1.0 µm) collection efficiencies expected during the field study. Significant increases in submicron particle collection efficiencies were measured between the new and used intake filters tested (23% and 98% efficiency) and the recirculation filters tested (12% and 76% efficiency). The rated submicron (0.3-1.0 µm) collection efficiency of the new MERV 16 intake and final filters were 95% and were assumed to be 98% for the used dust-loaded filters. Nearly 90 percent of the cab protection factor measurements were between the upper and lower modeled performance operating curves. The few data points observed outside the modeled ranges can be accounted for by slightly increasing or decreasing the filter efficiencies and air leakage variables by 1 to 2%. Thus, the three-filter model reasonably predicted the protection factor operating ranges for the changing filtration system characteristics during the seven-month field study. This three-filter system design also provided superior cab modeling results and robust long-term protection factor performance in the field as compared to the single- and two-filter systems modeled and studied in the laboratory.

DISCLAIMER

The findings and conclusions in this paper are those of the authors and do not necessarily represent the views of the National Institute for Occupational Safety and Health. Mention of any company name, product, or software does not constitute endorsement by NIOSH.

REFERENCES

1. ASAE (American Society of Agricultural Engineers). Agricultural cabs - environmental air quantity, Part 1: Definitions, test methods, and safety practices, ASAE Standard S525-1.1, St. Joseph Mich (1997).

2. ASHRAE (American Society of Heating, Refrigerating and Air-Conditioning Engineers). Method of Testing General Ventilation Air-Cleaning Devices for Removal Efficiency by Particle Size, Standard 52.2, Atlanta, GA (1999).

3. Cecala, A.B., Organiscak, J.A., Noll, J.D., Rider, J.P., 2013, "Key components for an effective filtration and pressurization system to reduce respirable dust in enclosed cabs for the mining industry," *Society of Mining, Metallurgy and Exploration, Inc.,* Englewood, CO, Pre-print 13-011, SME Annual Meeting, Feb. 24-27, 2013, Denver, CO, pp. 1-7.

4. Cecala, A.B., Organiscak, J.A., and Noll, J.D., 2012-A, "Long-term evaluation of cab particulate filtration and pressurization performance," *Society of Mining, Metallurgy and Exploration, Inc.,* Englewood, CO, Transactions 2012, Vol. 332, pp. 521- 531.

5. Cecala, A.B., O'Brien, A.D., Schall, J., Colinet, J.F., Fox, W.R, Franta, R.J., Joy, J., Reed, W.R, Reeser, P.W., Rounds, J.R., and Schultz, M.J., 2012-B, "Dust Control Handbook for Industrial Minerals Mining and Processing," Pittsburgh, PA: U.S. Department of Health and Human Services, Centers for Disease Control and Prevention, National Institute for Occupational Safety and Health, DHHS (NIOSH) Publication No. 2012-112, Report of Investigations 9689, pp. 1-284.

6. Cecala, A.B., Organiscak, J.A., Zimmer, J.A., Heitbrink, W.A., Moyer, E.S., Schmitz, M., Ahrenholtz, E., Coppock, C.C., and Andrews, E.H., 2005, "Reducing enclosed cab drill operators' respirable dust exposure with effective filtration and pressurization techniques," *Journal of Occupational and Environmental Hygiene*, Vol. 2, pp. 54-63.

7. Cecala, A.B., Organiscak, J.A., Heitbrink, W.A., Zimmer, J.A., Fisher, T., Gresh, R.E., and Ashley, J.D. II, 2004, "Reducing enclosed cab drill operator's respirable dust exposure at surface coal operations with a retrofitted filtration and pressurization system," *Society of Mining, Metallurgy and Exploration, Inc.,* Englewood, CO, Transactions 2003, Vol. 314, pp. 31-36.

8. Chekan, G.L., and Colinet, J.F., 2003, "Retrofit options for better dust control cab filtration, pressurization systems prove effective in reducing silica dust exposures in older trucks," *Aggregates Manager*, Vol. 8, No. 9, pp. 9-12.

9. Heitbrink, W.A., Thimons, E.D., Organiscak, J.A., Cecala, A.B., Schmitz, M., and Ahrenholtz, E., 2000, "Static pressure requirements for ventilated enclosures," In: Proceedings of the Sixth International Symposium on Ventilation for Contaminant Control, Helsinki, Finland, June 4-7, 2000, pp. 97-99.

10. NIOSH, 2008, "Minimizing Respirable Dust Exposure in Enclosed Cabs by Maintaining Cab Integrity," Technology News Bulletin No. 533, September 2008, DHHS (NIOSH) Publication No. 2008-147.

11. Noll, J., Cecala, A., and Organiscak, J., 2010, "The effectiveness of several enclosed cab filters and systems for reducing diesel particulate matter," *Society of Mining, Metallurgy and Exploration, Inc.,* Englewood, CO, Transactions 2010, Vol. 328, pp. 408-415.

12. Organiscak, J.A., and Cecala, A.B., 2009. "Doing the math–the effectiveness of enclosed-cab air–cleaning methods can be spelled out in mathematical equations," *Rock Products*, October, pp. 20–22.

13. Organiscak, J.A., and Cecala, A.B., 2008-A, "Laboratory investigation of enclosed cab filtration system performance factors," *Mining Engineering*, Vol.60, No. 12, pp. 74-80.

14. Organiscak, J.A., and Cecala, A.B., 2008-B, "Key design factors of enclosed cab dust filtration systems," Pittsburgh, PA: U.S. Department of Health and Human Services, Centers for Disease Control and Prevention, National Institute for Occupational Safety and Health, DHHS (NIOSH) Publication No. 2009-103, Report of Investigations 9677, pp. 1-43.

15. Organiscak, J.A., Cecala, A.B., Thimons, E.D., Heitbrink, W.A., Schmitz, M., and Ahrenholtz, E., 2004, "NOSH/Industry collaborative efforts show improved mining equipment cab dust protection," *Society of Mining, Metallurgy and Exploration, Inc.,* Englewood, CO, Transactions 2003, Vol. 314, pp. 145-152.